FUEL BUNDLE IMPACT VELOCITIES DUE TO REVERSE FLOW

N.N.WAHBA* and K.E.LOCKE**

*** Ontario Hydro, Reactor Safety and Operational Analysis Department
700 University Avenue, Toronto, Ontario, M5G-1X6**

**** Ontario Hydro, Bruce NGS A, Nuclear Safety Department
Bruce Township, Ontario, N0G-2T0**

ABSTRACT

If a break should occur in the inlet feeder or inlet header of a CANDU reactor, the rapid depressurization will cause the channel flow(s) to reverse. Depending on the gap between the upstream bundle and shield plug, the string of bundles will accelerate in the reverse direction and impact with the upstream shield plug. The reverse flow impact velocities have been calculated for various operating states for the Bruce NGS A reactors. The sensitivity to several analysis assumptions has been determined.

1. INTRODUCTION

In CANDU reactors, the fuel channels contain "strings" of 12 or 13 bundles, depending on the channel design. During normal operation, the channel flow forces the bundles in a channel towards the downstream end where they rest against either the downstream shield plug or fuel latch. A small gap, typically less than 0.1 m, exists between the end bundle and upstream shield plug. However, the gap increases over the lifetime of the reactor, due to pressure tube creep, and may become as large as 0.3 m. Also, during abnormal situations, and for a short period of time for single-ended refuelling modes, fewer than the full complement of bundles may be present in a channel and the gap can be significantly larger. When a break occurs in the upstream feeder, the rapid depressurization will cause the channel flow to reverse forcing the string of bundles to accelerate and impact with the upstream shield plug. The potential for bundle and channel damage depends on the bundle velocity at impact.

A series of five reverse flow, bundle acceleration experiments have been conducted at Stern Laboratories Inc., simulating a break in a 37-element, CANDU fuel channel for full power and zero power hot conditions [1,2]. The experimental apparatus consisted of a full scale reactor channel with end-fittings and feeders. The break was simulated using a rupture disc and bundle velocities were measured using a system of magnets and coils. The tests covered the range from a full complement of 13 bundles, with an initial bundle-to-shield plug gap of 0.202 m, to the case of 6 bundles missing with a gap of 3.172 m.

Similar behaviour was observed in all tests. The bundles were observed to accelerate rapidly at first and then level off to a constant or asymptotic value after a few hundred milliseconds, unless the transient is terminated by impact with the shield plug. The experiments show that the bundle string essentially moves as a unit. However, in one of the tests, there was an evidence of significant bundle separation due to high initial outlet temperature which resulted in a high voiding following rupture. Bundle separation would distribute the momentum transfer of the bundle to the shield plug over time which could lessen the damage to fuel bundles and fuel channel.

A model, SOPHT-RFI [2,3], which is a modification of the fully transient, two-phase thermal hydraulic code, SOPHT [4], has been developed to incorporate the interaction and feedback between bundle motion and channel thermal hydraulics. The model has been extensively modified to account for various forces acting on the bundle due to reverse flow [3]. These forces result from the pressure gradient, drag and friction between the bundles and the pressure tube. The calculational control volumes of nodes are adjusted to account for the location and velocity of the bundle.

The analytical model has been validated against the experiments. The agreement between measured and predicted velocities is excellent (less than 5.6 percent), for all tests with the exception of test 4 where the model over-predicts the impact velocity by about 28 percent. The over-prediction, in test 4, may be attributed to the analytical assumption that the bundles are considered as one solid string whereas the measurements indicated that a significant separation occurred among the first four bundles. The details of the code modifications as well as a comparison between measured and predicted values are given in Reference 3. It was also demonstrated that the model may be successfully used to simulate the thermal hydraulic and bundle movement in the fuel channel following large LOCA or, in the case of a guillotine break at the inlet feeder [3].

The bundle velocities depend on the reactor operating conditions such as channel power as well as coolant pressure and temperature. In this work four various operating states for Bruce NGS A, are considered. These states include full power, zero power, shutdown hot and shutdown cold. The initial temperature profile across the channel is flat for all cases, with the exception of the full power case. The outlet header pressure is relatively smaller (about 4 MPa) for shutdown cases than that (about 9 MPa) for full and zero power cases. Inlet header temperature is about 50°C for the shutdown cold case while it is about 260°C for the other cases.

The main parameters affecting the bundle movement due to reverse flow are discussed in Section 2. The analytical model is used to simulate the thermal hydraulic transient in a single channel and predict the bundle movement for a range of numbers of bundles missing in the channel. The analytical simulation is discussed in Section 3. Samples of results for a Bruce NGS A application are shown in Section 4. Summary and conclusions are presented in Section 5.

2. MAIN PARAMETERS AFFECTING BUNDLE MOVEMENT

The model may be used to simulate the thermal hydraulic transient and bundle movement in a single channel in the case of a guillotine break at the inlet feeder. The bundle motion depends, in general, on the reactor conditions, channel geometry as well as the size and location of the break, as discussed in Section 4. The main parameters that affect the bundle movement due to the flow reverse, are:

(1) The initial channel thermal hydraulic conditions including channel power and flow, pressure distribution, coolant temperature profile;
(2) The gap between the first bundle and the shield plug (nominal gap added to the length of the missing bundles);
(3) The location of the break (distance between the break and the inlet end-fitting);
(4) The size of the break (diameter of the inlet feeder);
(5) The length and flow resistance of the outlet feeder;
(6) The end-fittings characteristics;
(7) The mass of fuel bundle; and
(8) The friction between the bundles and the pressure tube.

3. IMPACT VELOCITY FOLLOWING A GUILLOTINE BREAK AT THE INLET FEEDER

The model is used in predicting the impact velocity and kinetic energy following a guillotine break at the inlet feeder for Bruce NGS A under various reactor operating states such as:

(1) Shutdown Hot , Pressurized to 4 MPa, 4 HT Pumps Running;
(2) Shutdown Cold , Pressurized to 4 MPa, 4 HT Pumps Running;
(3) Zero Power Hot; and
(4) Full Power.

3.1 Analytical Simulation

The header conditions for the various reactor states such as pressure, temperature and enthalpy were calculated using the SOPHT circuit model for Bruce NGS A and are listed in Table 1. During the transient, the outlet header pressure and enthalpy are used as fixed constant boundary conditions. To select appropriate channels for the calculations, the thermohydraulic conditions of all channels were calculated at zero power using the computer code NUCIRC-II [5]. Based on these calculations, channels M04 and C12, with a minimum outlet feeder resistance and having the largest inlet feeder cross-sectional area of 0.0031114 m^2, were selected to represent the inner and outer zones, respectively. They are expected to have maximum impact velocity. The gap between the end bundle and the shield plug is assumed to be 0.3 m when all of the thirteen bundles are present. The mass of each bundle is 23.7 kg.

The channel, feeders and end-fittings are finely nodalized. The channel was modelled using two multi-node modules. One module represented the section of the channel occupied by the bundles and the other module represented the section of empty channel. The end-fittings were modelled as an annulus representing the direct flow path between the liner tube and end-fitting wall. The appropriate form loss factors for the various pipe sections of the feeders, end-fittings and channel are used. In the case of a channel with less than the full complement of bundles, the channel power is adjusted accordingly.

The guillotine break at the inlet feeder was assumed to occur just upstream of the inlet end-fitting. This maximizes the pressure drop across the bundle string and consequently, results in the highest bundle velocity. The break was simulated by two break discharge valves and an externally controlled varying resistance link. This resistance link is assigned a large value after the break to cut off flow between the two segments of the feeder at the break location so that the coolant is discharged to atmosphere through the discharge valve.

4. RESULTS AND DISCUSSIONS

The predicted void transients at five fixed locations along the inner zone channel having 6 bundles missing, are illustrated in Figure 1, for the case of Full Power. Initially, there is no void in the channel. At the onset of the break the void, at the break location (represented by the solid line in Figure 1), starts to increase rapidly due to the sudden reduction in the pressure at this location. Then the void decreases for the rest of the transient. At the end of the transient, the break void increases again as the void at the outlet end is transferred toward the inlet. Figure 1 shows also, the void transient at other locations, namely, downstream node (initial position of the downstream bundle), middle node (initial location of the middle bundle), upstream node (initial position of the upstream bundle), and gap node just downstream of the inlet end-fitting. It can be seen that the void front moves toward the inlet with further void generation because the channel remains at full power. At a fixed location, the void collapses after the last (downstream) bundle passes by this location.

The forces acting on the bundle include: the pressure force, drag force, friction force due to friction between bearing pads and pressure tube. The positive direction of the bundle displacement, velocity and acceleration, coolant flow and forces acting on the bundle, is assumed to coincide with the direction from outlet to inlet feeders. The predicted transient forces, for the inner zone channel with 6 bundles missing in the case of full power, are shown in Figure 2. The pressure force arises from the pressure difference at the two ends of the bundle, and acts on the cross-sectional area of the bundle. At the onset of the break, the pressure at the break drops to the saturation pressure corresponding to the inlet header temperature and this results in a large initial pressure force, as shown in Figure 2, which accelerates the bundle string. The drag force is caused by the frictional force exerted by the coolant flowing past the bundle. After the initial forward flow momentum is overcome by the flow reversal, the drag force increases to reach a limiting value and then starts to decrease. The pressure and drag forces are proportional to the square of the relative velocity between the coolant and the bundle. Therefore, both forces decrease in the later portion of the transient, as shown in Figure 2. The friction force due to the contact between the bundles and the pressure tube, is proportional to the weight of the bundle, acts in the opposite direction of the bundle movement and is relatively smaller than the pressure force or the drag force, as illustrated in Figure 2.

The net resultant force is used in the calculations of the bundle acceleration. In the following sub-sections, the predicted transient bundle velocities and kinetic energy, at impact, following a guillotine break at the inlet feeder, are discussed for each reactor operating state considered.

4.1 Shutdown Hot, Pressurized to 4 MPa, 4 HT Pumps Running

The calculations were carried out for different numbers of missing bundles in the inner zone channel. The bundle velocities as functions of time, are shown in Figures 3 to 5. The bundle string accelerates rapidly at first and then levels off and starts to decelerate gradually (as shown in Figure 5, for 10 or more missing bundles), unless the transient is terminated by impact with the shield plug (as shown in Figures 3 and 4, for smaller numbers of missing bundles). The driving force and consequently the acceleration of the fuel bundles are proportional to the pressure drop across the bundle string and the drag force acting on it. Both forces are proportional to the square of the relative velocity of the coolant flowing through the bundles, i.e., coolant velocity less bundle velocity. As the bundle string accelerates, the relative velocity and therefore the accelerating force, decreases and the bundle string asymptotically approaches a limiting velocity. In cases where only a few bundles are missing from the channel, the bundles may hit the shield plug well before reaching the asymptotic velocity as shown in Figures 3 and 4.

The initial forward flow momentum may delay the bundle initial acceleration and the onset of the bundle motion as shown in Figures 3 to 5. At the onset of the break, the inlet pressure (at the break location), drops to the saturation pressure (about 3.7 MPa), corresponding to the inlet header temperature which results in a relatively small pressure drop across the bundle string since the outlet header pressure is about 4.0 MPa.

The impact velocity is mainly governed by the bundle/shield plug gap which limits the time over which the bundles can accelerate. The larger the gap, the greater the time available for acceleration. The fewer bundles in the channel, the larger the gap and the higher the impact velocity unless the bundles reach the asymptotic limit. The impact velocity as well as kinetic energy for various missing bundles are given in Table 2. The maximum impact velocity is 8.45 m/s and corresponds to the case of eight missing bundles (i.e. five bundles are present). Increasing the number of missing bundles beyond this value results in a lower impact velocity. In this case, the bundle string reaches the limiting velocity and starts to decelerate before the end of the transient. It can also be concluded that operating with five missing bundles (i.e. eight bundles are present) yields the largest kinetic energy of 5.45 kJ, at impact, corresponding to impact velocity of 7.58 m/s.

4.2 Shutdown Cold, Pressurized to 4 MPa, 4 HT Pumps Running

For the case of Shutdown Cold, the bundle velocities as functions of time, for various numbers of missing bundles in the inner zone channel, are shown in Figure 6. In this case, the bundle string starts to move earlier and with a greater initial acceleration compared to the case of Shutdown Hot. This is due to the fact that the inlet header temperature, for the Shutdown Cold case, is significantly lower than that for the Shutdown Hot case. Since the outlet header pressures are almost equal for both cases, the pressure drop across the bundle string as well as the discharged flow and the drag force and consequently the initial driving force and acceleration are greater for the Shutdown Cold case than the Shutdown Hot case.

As the number of missing bundles increases, the driving forces may decrease because of lower loss coefficient and consequently lower pressure drop and drag forces acting on the bundle string. However, this effect is compensated by lower total mass of the bundle string. Therefore, the number of missing bundles has a small effect on the transient of the bundle motion as shown in Figure 6.

The impact velocity is determined by the bundle/shield plug gap. The fewer bundles in the channel, the larger the gap and the impact velocity as long as the bundles do not reach the asymptotic value. The impact velocity and kinetic energy are listed in Table 3. The case of two missing bundles. has the maximum kinetic energy of 5.49 kJ at impact., corresponding to impact velocity of 6.49 m/s.

4.3 Zero Power Hot

For the case of Zero Power Hot, the bundle velocities as functions of time, for various numbers of missing bundles, are shown in Figures 7 and 8 for inner and outer zones, respectively. As the number of missing bundles increase, the bundle velocity is slightly larger during the transient.

Although the difference in inlet header conditions between inner and outer zones, is insignificant, the bundle velocity is larger for the outer zone channel than the inner zone channel. This is because the outlet feeder of the outer zone channel C12 has lower flow resistance than that of the inner zone channel M04 which yields a larger pressure drop and driving force acting on the bundle string for the outer zone channel than the inner zone channel.

The impact velocity as well as kinetic energy for various missing bundles are given in Tables 4 and 5 for inner and outer zones, respectively. The impact velocity and consequently kinetic energy are larger in the Zero Power Hot case than in the Shutdown cases due to the larger driving (outlet header) pressure. For Zero Power Hot conditions, operating with three and four missing bundles (i.e. ten and nine bundles are present) yields the largest kinetic energies of 10.45 and 11.83 kJ, at impact, corresponding to impact velocities of 9.39 and 10.53 m/s for inner and outer zones, respectively.

4.4 Full Power

For the case of Full Power, the bundle velocities as functions of time, for various numbers of missing bundles, for 0 to 8 missing bundles, are shown in Figures 9 and 10 for inner and outer zones, respectively. At the onset of the break, the pressure at the break location drops to the saturation pressure corresponding to the inlet header temperature and the initial pressure gradient accelerates the bundle string. Since the outer zone inlet header temperature is larger than that of the inner zone, the pressure gradient and the initial acceleration are larger for the inner zone case than the outer zone case. The initial stage is followed by a second stage where the acceleration decreases as the bundles start to move. The second stage starts earlier as the number of missing bundles increases, as shown in Figures 9 and 10. Then the velocity changes slope and increases again. The reason of this change in the acceleration is due to the transient void and pressure. In some cases (8 missing bundles), a maximum velocity is reached prior to the impact whereas in others, the transient is terminated by impact with the shield plug.

The impact velocity as well as kinetic energy for various missing bundles are given in Tables 6 and 7 for inner and outer zones, respectively. In this case, operating with six missing bundles (i.e. seven bundles are present) yields the largest kinetic energies of 14.17 and 13.42 kJ, at impact, as well as the largest impact velocities of 13.07 and 12.72 m/s for inner and outer zones, respectively. Although the outlet feeder of the outer zone channel C12 has lower flow resistance than that of the inner zone channel M04, the bundle velocity is larger for the inner zone channel than the outer zone channel. This is because the inlet header temperature is higher and consequently the pressure drop across the bundle string is smaller for the outer zone channel case than the inner zone case.

4.5 Sensitivity Study

The sensitivity of the impact velocity to various parameters is investigated. In these calculations the following cases (having maximum kinetic energy at impact) are considered:

(1) Full Power (Inner Zone) with 6 bundles missing;
(2) Full Power (Outer Zone) with 6 bundles missing;
(3) Zero Power Hot (Inner Zone) with 3 bundles missing;
(4) Zero Power Hot (Outer Zone) with 4 bundles missing;
(5) Shutdown Hot (Inner Zone) with 5 bundles missing; and
(6) Shutdown Cold (Inner Zone) with 2 bundles missing.

The sensitivity of the impact velocity to the following parameters are listed in Table 8:

4.5.1 Inlet Feeder Diameter

The break flow is likely limited by two-phase choking in the inlet feeder piping rather than in the inlet end-fitting because the minimum flow area in the end fitting is greater than in the feeder pipe. Impact velocities are expected to be greater for the larger pipe because of the greater discharge flow

The reference calculations were carried out using the largest inlet feeder diameter of 2.5" (corresponds to flow area of 0.0031114 m^2)to maximize the reversed flow and consequently the impact velocity. In the sensitivity study, inlet feeder diameter of 2.0" (corresponds to flow area of 0.0018777 m^2) is used. The value of the impact velocity becomes smaller as the inlet feeder diameter decreases as shown in Table 8(a). It can also be concluded that this sensitivity depends largely on the thermohydraulic conditions and channel geometry.

4.5.2 Outlet Feeder Resistance

The reference calculations were carried out using the channel with minimum outlet feeder resistance in both inner and outer zones. To confirm that this simulation yields the maximum impact velocity, the outlet feeder loss factor is increased by 1.0 and the results are given in Table 8(b).

The effect of outlet feeder resistance is less pronounced in the case of Shutdown-Cold since the outlet header temperature is very small and no void is expected in the outlet feeder which yields a smaller pressure drop across the outlet feeder.

4.5.3 Outlet End-fitting Resistance

The flow resistance of the end-fitting would be somewhat reduced causing higher bundle velocity if the inlet shield plug assembly was removed. In this sensitivity study, only the annulus resistance is considered whereas the loss factor of the shield plug is assumed to be zero. The reduction in the outlet end-fitting resistance results in larger impact velocity by less than 15% as shown in Table 8(c).

4.5.4 Inlet Header Temperature

The channel inlet pressure transient is controlled by the break discharge flow and upstream thermohydraulics. The discharge (choked flow) is strongly dependent on the upstream coolant temperature and void. The minimum pressure to which the inlet feeder drops is directly related to the initial temperature, i.e., the lower the initial temperature, the lower the pressure and the larger the driving forces acting on the bundle string. The pressure at the inlet end of the channel falls to saturation pressure of inlet header temperature and later increases when the higher temperature coolant from the outlet end flows through the channel.

In this case, the inlet header temperature was reduced by 4 and 2°C for inner and outer zones, respectively. These reductions result in an increase of the impact velocity by about 2 and 1% for inner and outer zones, respectively, for Full Power case. The results are given in Table 8(d).

5. SUMMARY AND CONCLUSIONS

During normal operation, the channel flow forces the bundle string towards the downstream end where they rest against the fuel latch. A small gap exists between the end bundle and upstream shield plug. When a fewer than the full complement of bundles are present in a channel, the gap is larger. In the event that a break occurs in the inlet feeder or inlet header, the rapid depressurization will cause the channel flow to reverse forcing the string of bundles to accelerate and impact with upstream shield plug. In this case, the potential bundle and channel damage depends primarily on the velocity of the bundles at impact. Removal of one or more of the inlet end bundles would add a gap equal to the length of these bundles to the existing gap and may result in a larger impact velocity.

The reverse flow impact velocities, in the case of a guillotine break at the inlet feeder, are determined for Bruce NGS A under various reactor operating states using the validated model SOPHT-RFI. The information is needed to support operation with less than a full complement of bundles in the channel and is also required to support channel defuelling. The impact velocities may be used to evaluate channel component integrity analysis.

The maximum kinetic energies, at impact, are 5.45, 5.49, 10.45, 11.83, 14.17 and 13.42 kJ (corresponding to impact velocities of 7.58, 6.49, 9.39, 10.53, 13.07 and 12.72 m/s) for the cases of Shutdown Hot (inner zone), Shutdown Cold (inner zone), Zero Power Hot (inner zone), Zero Power Hot (outer zone), Full Power (inner zone) and Full Power (outer zone), respectively. The selected channels with minimum outlet feeder resistance and largest inlet feeder diameter give the largest impact velocity. Reducing the outlet end-fitting resistance or inlet header temperature yields larger impact velocity.

6. REFERENCES

[1] HADALLER,G.I. and SANDIG,P.F., "Reverse Flow Induced Bundle Impact Velocity Tests", Report SL-020, Stern Laboratories Inc., August 1995.

[2] LOCKE,K.E. and TRAN,F.B.P., "Thermal Hydraulic and Dynamic Modelling of Reverse Flow Bundle Acceleration Experiments", Ontario Hydro, Nuclear Safety Department, Report No. 90331, 1992.

[3] WAHBA,N.N. and O.Akalin, "Fuel Bundle Movement due to Reverse Flow", 16th Annual Conference, Canadian Nuclear Society, Saskatoon, June 4-7, 1995.

[4] CHANG,Y.F., "Thermal-Hydraulic System Simulation Model for the Reactor, Boiler and Heat Transport System (SOPHT)", Ontario Hydro Report, CNS-37-2, September, 1977.

[5] WAHBA,N.N. and J.A.Lorenc, "NUCIRC-II: A Computer Code for Nuclear Heat Transport Circuit Thermohydraulic Analysis ", Ontario Hydro, Design and Development Division, Report No. 84426, 1984.

TABLE 1
AVERAGE HEADER CONDITIONS

	Shutdown Hot	Shutdown Cold	Zero Power Hot	Full Power
Inlet Header (Inner Zone)				
Pressure (MPa)	5.1866	5.5286	10.3406	10.3715
Temperature (°C)	245.30	49.89	258.06	259.06
Enthalpy (kJ/kg)	1029.32	196.54	1089.24	1093.0
Inlet Header (Outer Zone)				
Pressure (MPa)	5.3351	5.7092	10.5375	10.5279
Temperature (°C)	245.30	49.86	259.01	269.43
Enthalpy (kJ/kg)	1029.32	196.54	1092.73	1142.9
Outlet Header				
Pressure (MPa)	3.9964	4.0004	9.18	9.18
Temperature (°C)	245.30	50.47	259.44	303.13
Enthalpy (kJ/kg)	1029.32	197.77	1095.10	1317.85

TABLE 2
SHUTDOWN-HOT, INNER ZONE CASE

Number of Missing Bundles	Impact Velocity (m/s)	Kinetic Energy (kJ)
0	2.40	0.89
1	4.21	2.52
2	5.38	3.77
3	6.22	4.58
4	6.95	5.15
5	7.58	5.45
6	8.04	5.36
7	8.34	4.95
8	8.45	4.23
9	8.43	3.37
10	8.29	2.44
11	7.69	1.40
12	6.52	0.50

TABLE 3
SHUTDOWN-COLD, INNER ZONE CASE

Number of Missing Bundles	Impact Velocity (m/s)	Kinetic Energy (kJ)
0	3.47	1.85
1	5.36	4.09
2	6.49	5.49
3	6.76	5.42
4	6.78	4.90
5	6.82	4.41
6	6.47	3.47

TABLE 4
ZERO POWER HOT, INNER ZONE CASE

Number of Missing Bundles	Impact Velocity (m/s)	Kinetic Energy (kJ)
0	4.40	2.98
1	6.98	6.93
2	8.38	9.15
3	9.39	10.45
4	9.82	10.28
5	10.09	9.65
6	10.24	8.70
7	10.19	7.38
8	10.13	6.08

TABLE 5
ZERO POWER HOT, OUTER ZONE CASE

Number of Missing Bundles	Impact Velocity (m/s)	Kinetic Energy (kJ)
0	4.75	3.48
1	7.45	7.89
2	9.01	10.58
3	9.95	11.73
4	10.53	11.83
5	10.93	11.32
6	10.79	9.66

TABLE 6
FULL POWER, INNER ZONE CASE

Number of Missing Bundles	Impact Velocity (m/s)	Kinetic Energy (kJ)
0	5.15	4.09
1	6.60	6.19
2	8.37	9.13
3	9.36	10.38
4	9.98	10.62
5	11.56	12.67
6	13.07	14.17
7	12.53	11.16
8	10.16	6.12

TABLE 7
FULL POWER. OUTER ZONE CASE

Number of Missing Bundles	Impact Velocity (m/s)	Kinetic Energy (kJ)
0	4.56	3.20
1	5.82	4.82
2	7.12	6.61
3	8.36	8.28
4	9.40	9.42
5	11.32	12.15
6	12.72	13.42
7	12.23	10.63
8	9.27	5.09

TABLE 8
SENSITIVITY OF IMPACT VELOCITY (m/s) TO VARIOUS PARAMETERS

(a) Inlet Feeder Diameter

	Reference Case	Sensitivity Case
Full Power (Inner Zone)	13.07	12.90
Full Power (Outer Zone)	12.72	9.15
Zero Power Hot (Inner Zone)	9.39	8.69
Zero Power Hot (Outer Zone)	10.53	10.11
Shutdown Hot (Inner Zone)	7.58	5.34

(b) outlet Feeder Resistance

	Reference Case	Sensitivity Case
Full Power (Inner Zone)	13.07	12.69
Full Power (Outer Zone)	12.72	12.10
Zero Power Hot (Inner Zone)	9.39	8.66
Zero Power Hot (Outer Zone)	10.53	10.07
Shutdown Hot (Inner Zone)	7.58	7.45
Shutdown Cold (Inner Zone)	6.49	6.48

(c) Outlet End-fitting Resistance

	Reference Case	Sensitivity Case
Full Power (Inner Zone)	13.07	13.96
Full Power (Outer Zone)	12.72	13.96
Zero Power Hot (Inner Zone)	9.39	10.29
Zero Power Hot (Outer Zone)	10.53	12.03
Shutdown Hot (Inner Zone)	7.58	7.74
Shutdown Cold (Inner Zone)	6.49	6.80

(d) Inlet Header Temperature

	Reference Case	Sensitivity Case
Full Power (Inner Zone)	13.07	13.36
Full Power (Outer Zone)	12.72	12.85

FIGURE 1: VOID FRACTION VS TIME
FULL POWER, INNER ZONE CASE (6 BUNDLES MISSING)

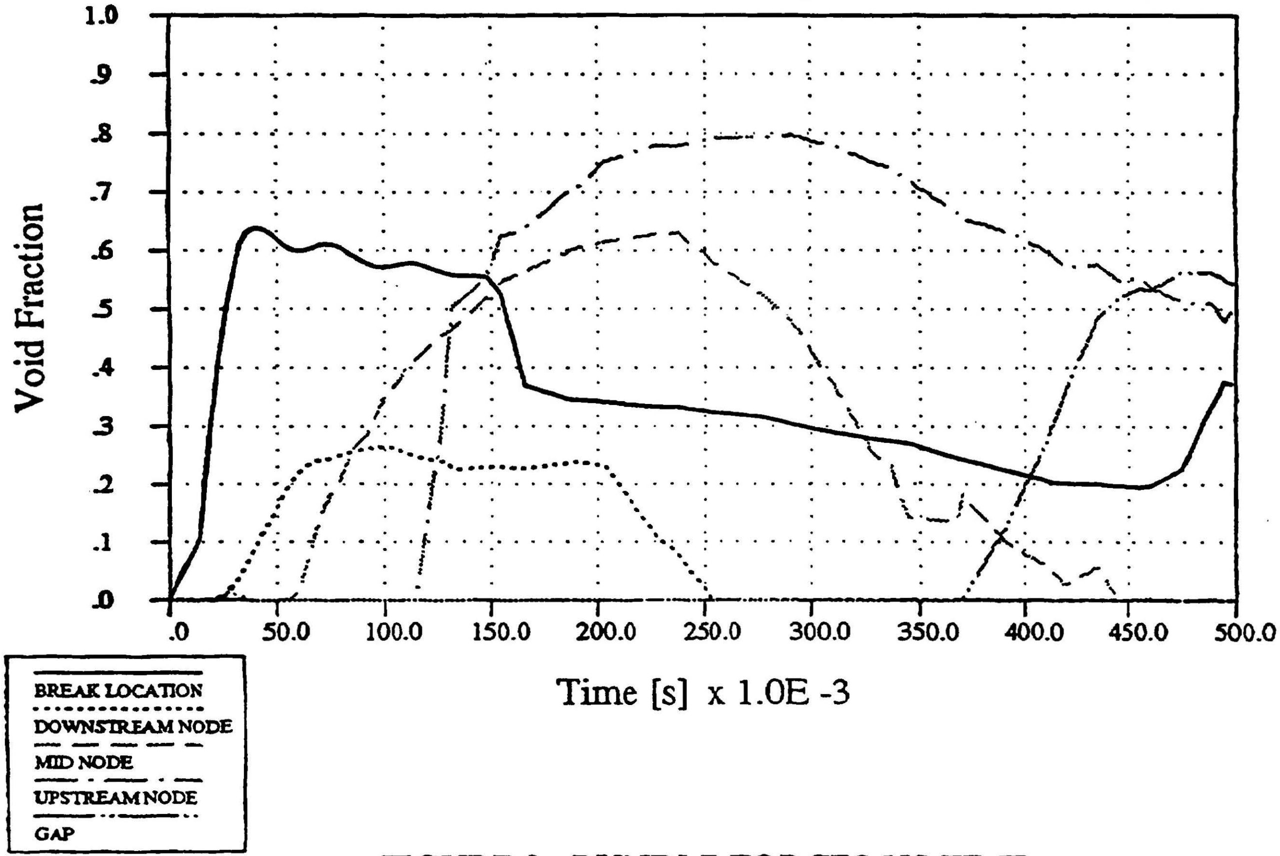

FIGURE 2: BUNDLE FORCES VS TIME
FULL POWER, INNER ZONE CASE (6 BUNDLES MISSING)

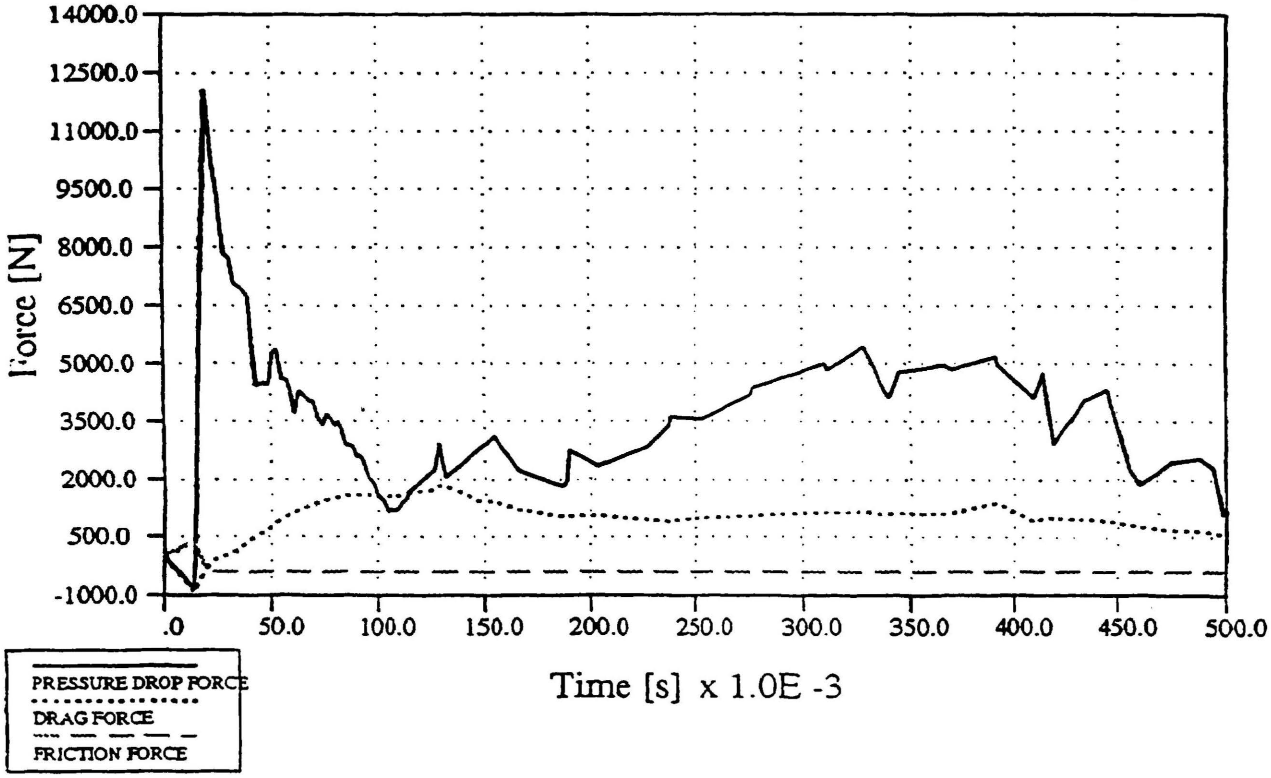

FIGURE 3: BUNDLE VELOCITY VS TIME
SHUTDOWN-HOT, INNER ZONE CASE

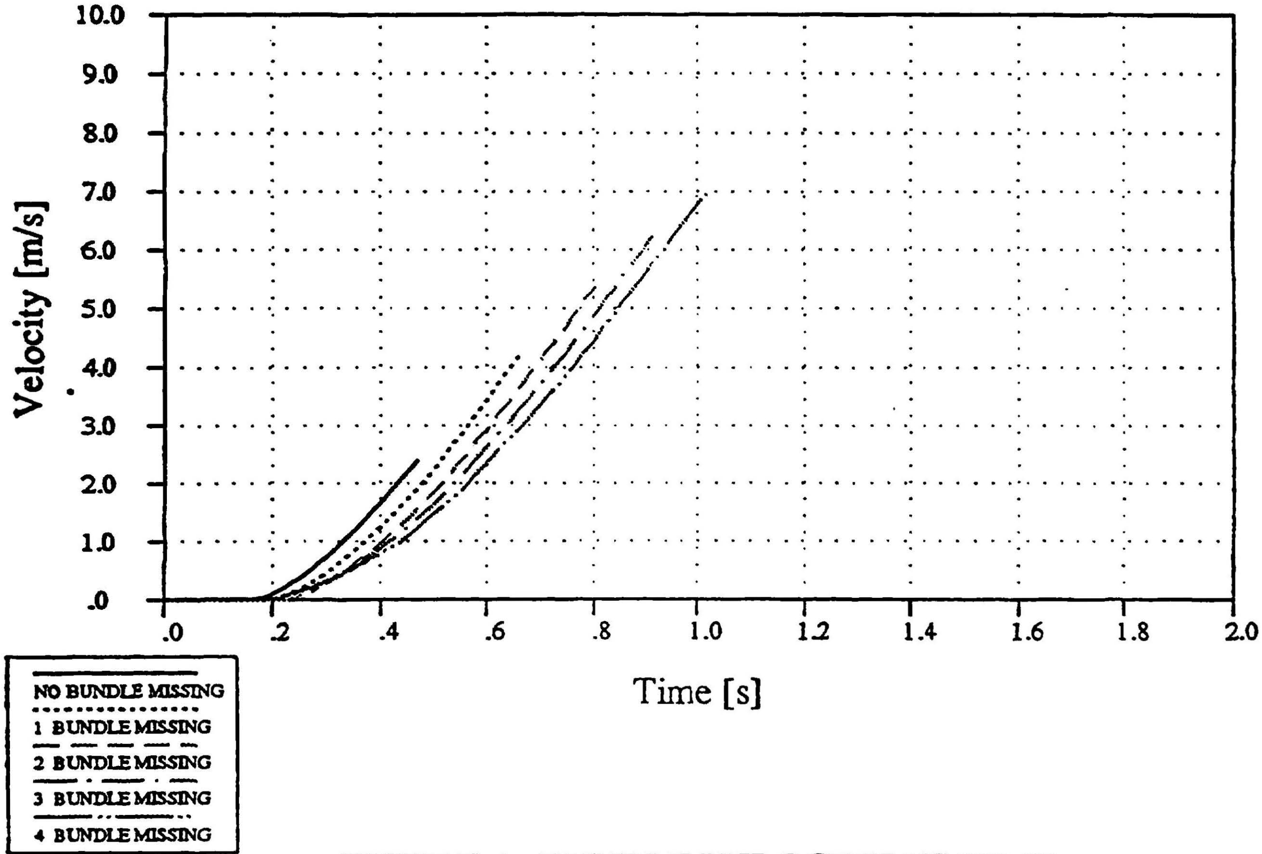

FIGURE 4: BUNDLE VELOCITY VS TIME
SHUTDOWN-HOT, INNER ZONE CASE

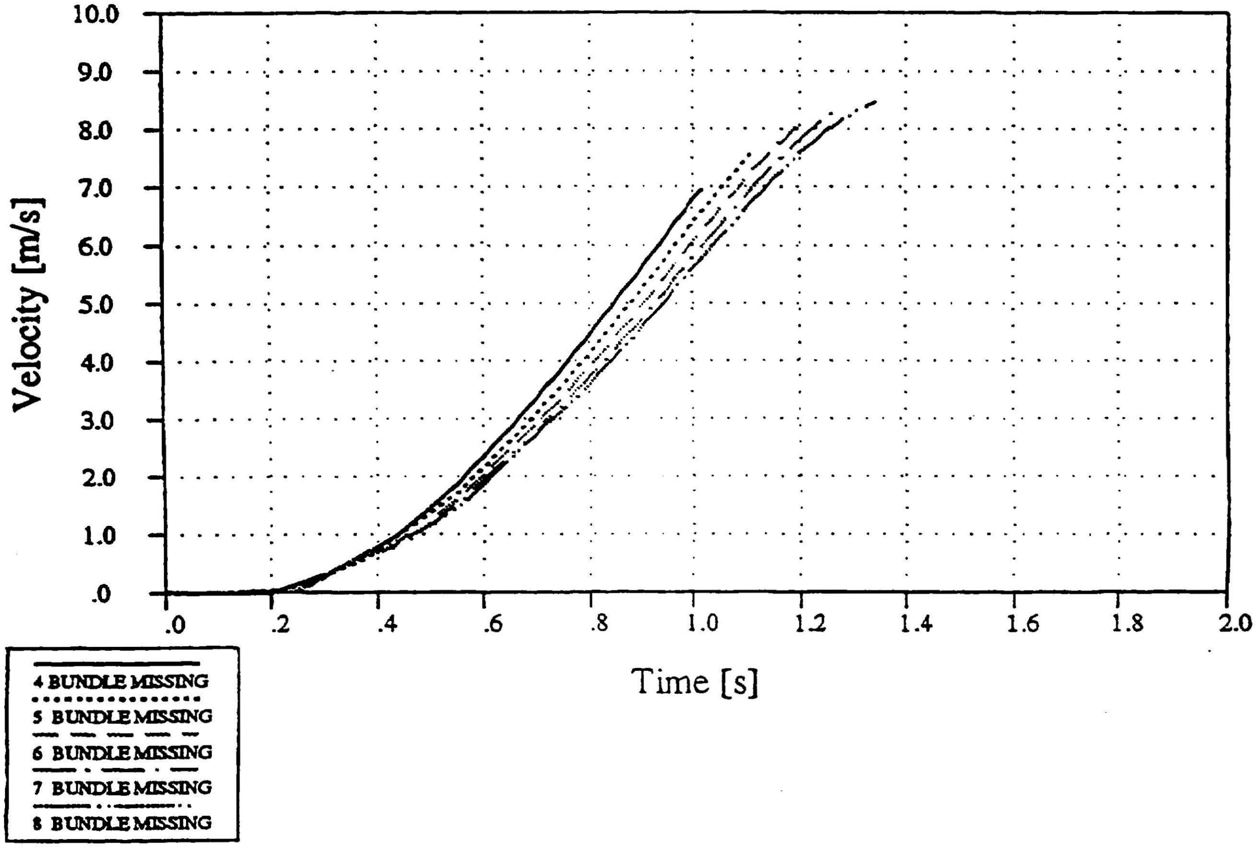

Mon Apr 22 14:53:14 1996
nwahta/II/A/ph.xls

FIGURE 5: BUNDLE VELOCITY VS TIME
SHUTDOWN-HOT, INNER ZONE CASE

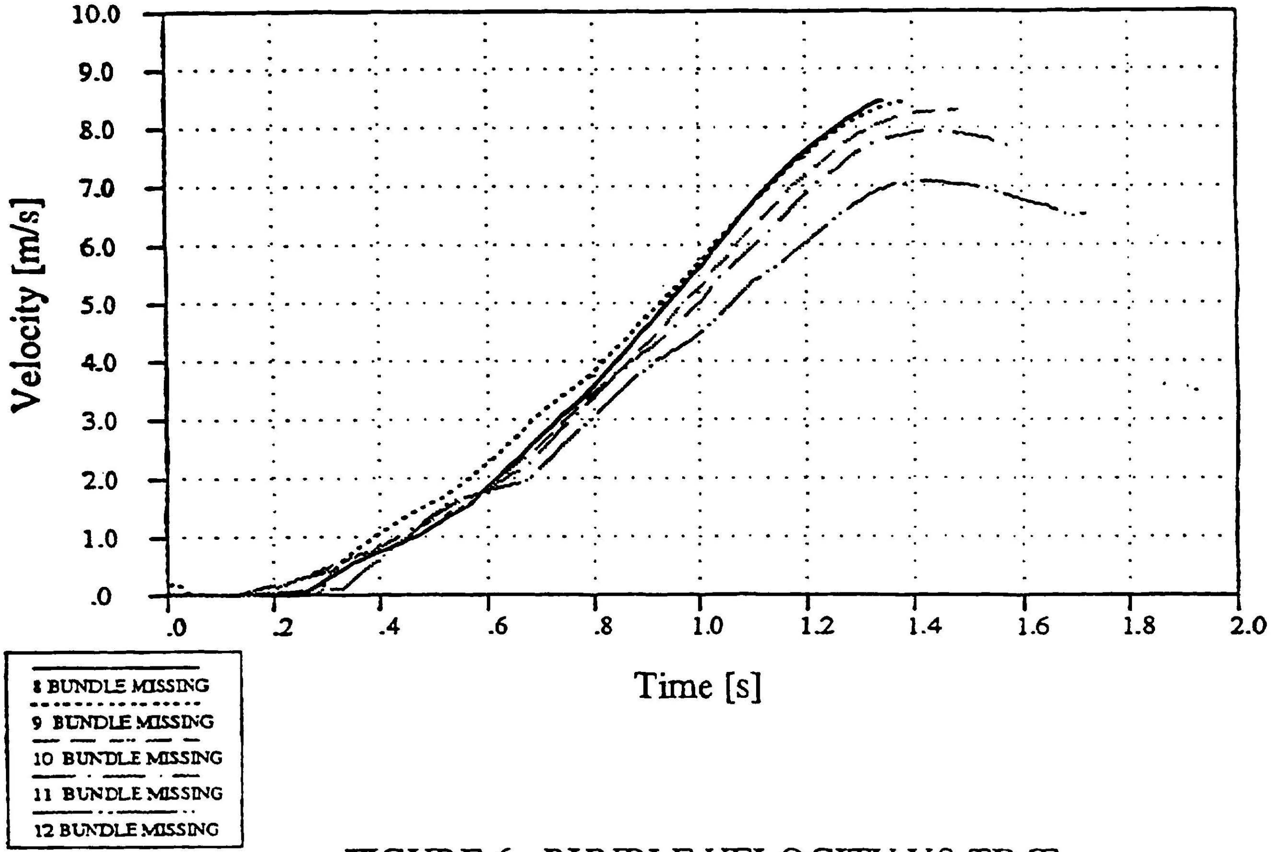

FIGURE 6: BUNDLE VELOCITY VS TIME
SHUTDOWN-COLD, INNER ZONE CASE

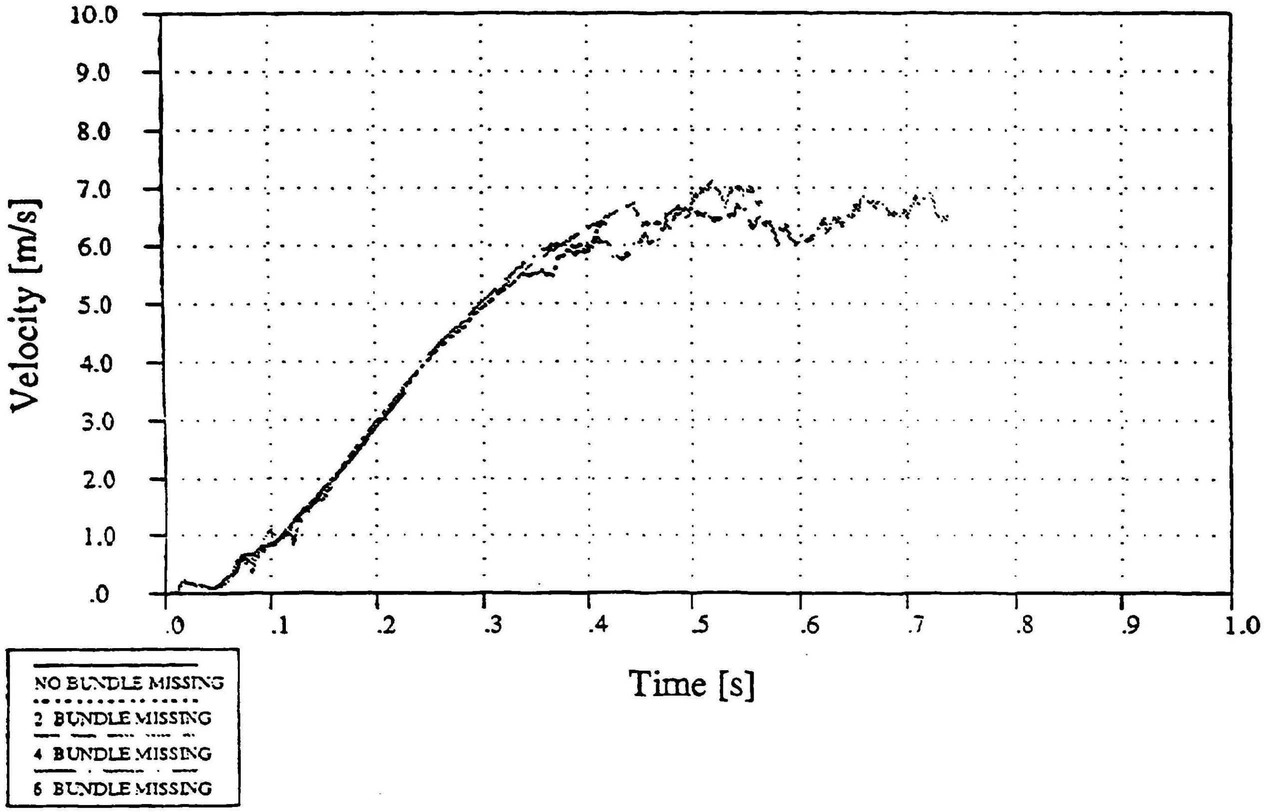

Mon Apr 22 14:54:50 1996

FIGURE 7: BUNDLE VELOCITY VS TIME
ZERO POWER-HOT, INNER ZONE CASE

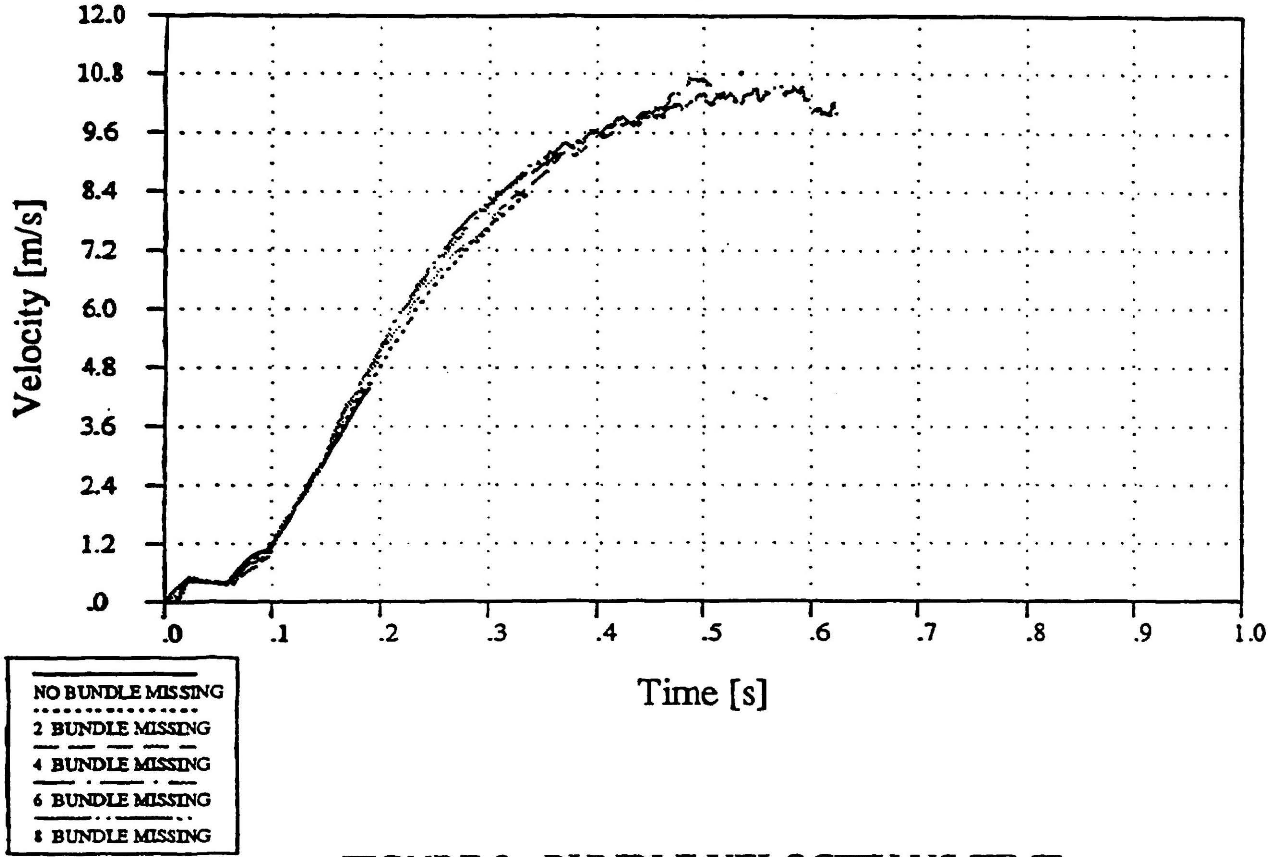

FIGURE 8: BUNDLE VELOCITY VS TIME
ZERO POWER-HOT, OUTER ZONE CASE

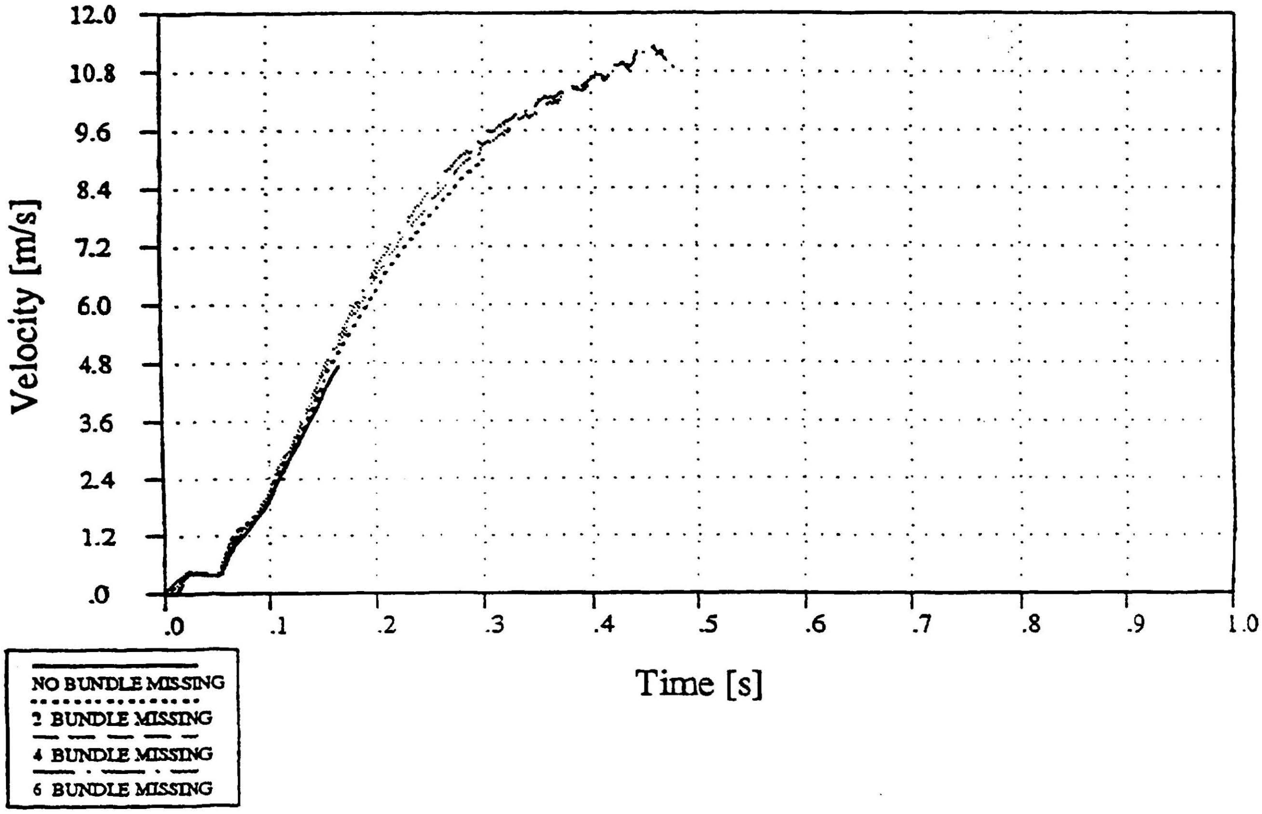

FIGURE 9: BUNDLE VELOCITY VS TIME
FULL POWER, INNER ZONE CASE

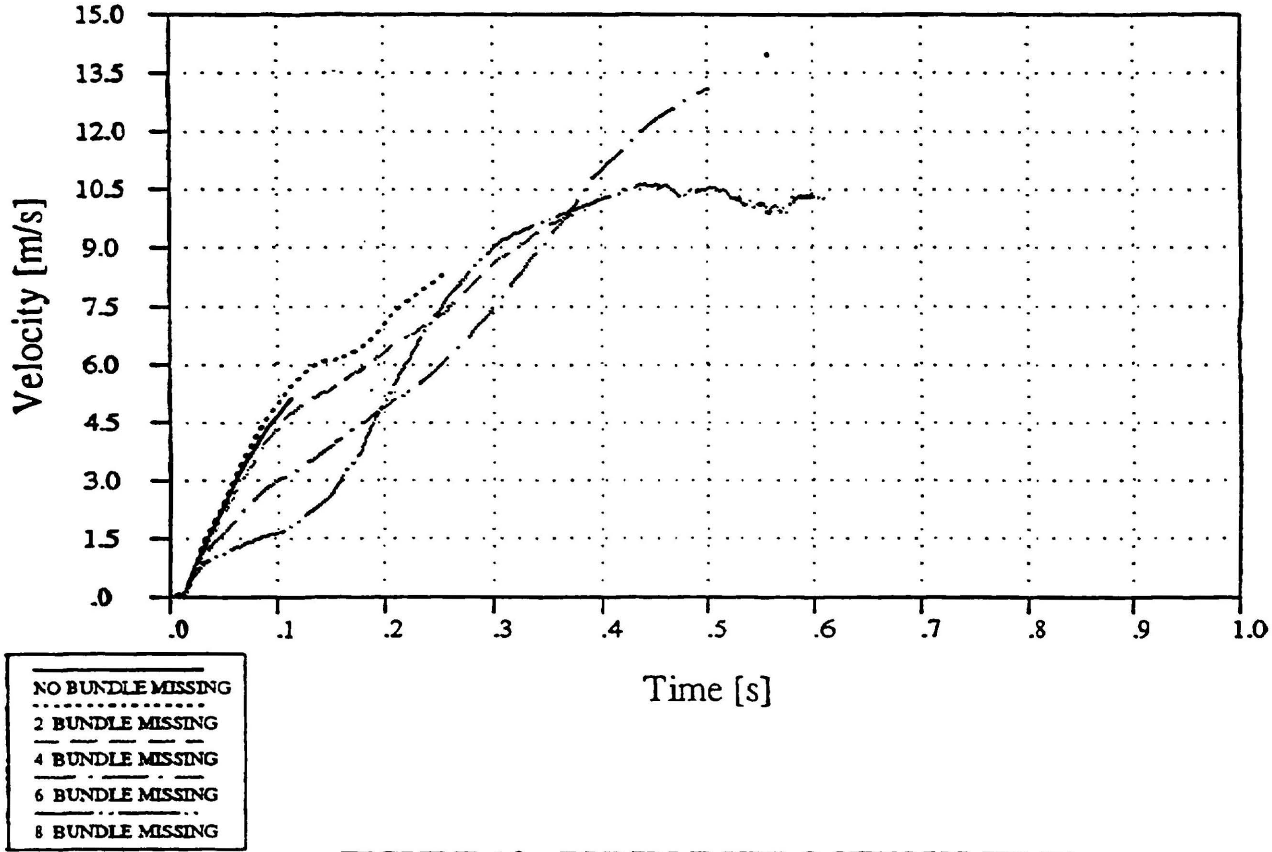

FIGURE 10: BUNDLE VELOCITY VS TIME
FULL POWER, OUTER ZONE CASE

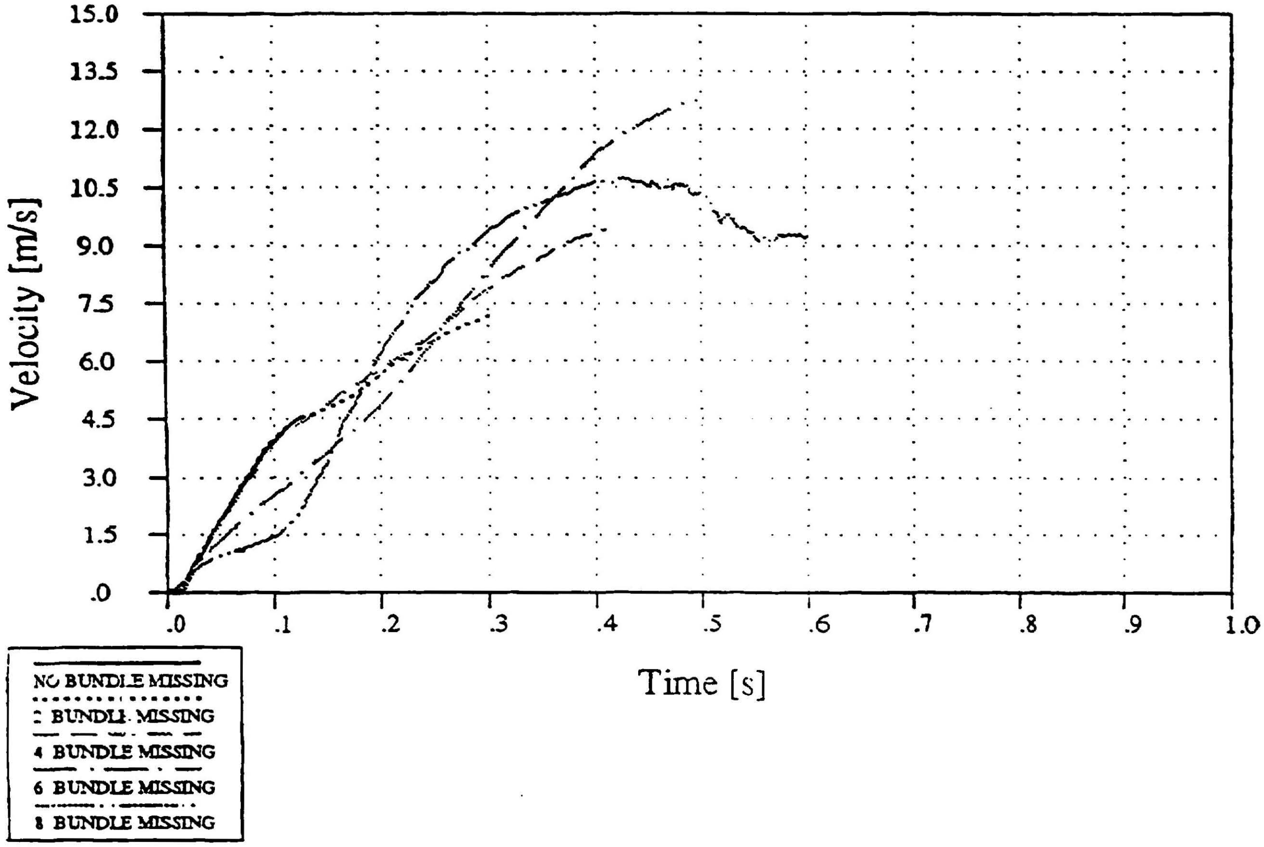

Mon Apr 22 14:58:01 1996